

Restoration of Halftoned Color-Quantized Images Using Projection Onto Convex Sets

Yik-Hing Fung and Yuk-Hee Chan

Centre for Multimedia Signal Processing
Department of Electronic and Information Engineering
The Hong Kong Polytechnic University, Hong Kong

ABSTRACT

Restoration of color-quantized images is rarely addressed in the literature especially when the images are color-quantized with halftoning. Direct applications of existing restoration techniques are generally inadequate to deal with this problem. In this paper, we propose a POCS-based restoration algorithm to solve the problem. This algorithm derives useful information for restoration with the available color palette and the mechanism of a halftoning process. It is shown to be able to provide a good restoration result.

1. INTRODUCTION

Color quantization is a process for reducing the number of colors in a digital image by replacing them with a representative color selected from a palette [1-4]. It is widely used to lessen the burden of massive image data on storage and transmission bandwidth in many multimedia applications. However, color quantization introduces artifacts such as false contour and color shift in the color-quantized images.

Digital halftoning [5,6] would be helpful to eliminate these defects by making use of the fact that human eyes act as spatial low-pass filters. The quantization error of a pixel after color quantization is diffused to neighboring pixels so as to hide the defects. At the moment, the most popular halftoning method is error diffusion and several well-known error diffusion filters such as Floyd-Steinberg and Stucki filters are generally used to achieve the goal[5].

Color quantization is a kind of degradation and restoration algorithms for recovering the original image from its color-quantized version is sometimes necessary. However, though there are a lot of reported works on the restoration of noisy and blurred color images [7-14], little effort has been seen in the literature for restoring halftoned color-quantized images. Obviously, the degradation models of the two cases are different and hence direct adoption of conventional restoration algorithms does not work effectively. Recently, a restoration algorithm for handling color-quantized images has been proposed, but it does not take care of the case when halftoning is involved in the quantization process[15]. This paper is devoted to formulating the process of color quantization when error

diffusion is involved and developing a POCS-based restoration algorithm to restore corresponding degraded images.

2. COLOR QUANTIZATION

A 24-bit full color image \mathbf{X} generally consists of three 8-bit color planes, say, \mathbf{X}_r , \mathbf{X}_g and \mathbf{X}_b , which represents the red, the green and the blue color planes of the image respectively. A pixel is then a vector represented as $\bar{\mathbf{X}}_{(i,j)} = (\mathbf{X}_{(i,j)r}, \mathbf{X}_{(i,j)g}, \mathbf{X}_{(i,j)b})$ for $0 < i, j \leq N$, where $\mathbf{X}_{(i,j)c} \in [0,1]$ is the intensity value of the c^{th} color component of the $(i,j)^{\text{th}}$ pixel. Here, we assume that the image is of size $N \times N$ and the maximum and the minimum intensity values of a pixel are, respectively, normalized to be 1 and 0.

Figure 1 shows the system which performs color quantization with halftoning. The input image \mathbf{X} is scanned in a row-by-row fashion from pixel (1,1) to pixel (N,N) and processed as follows to produce the encoded image \mathbf{Y} .

$$\mathbf{U}_{(i,j)c} = \mathbf{X}_{(i,j)c} - \sum_{(k,l) \in S} \mathbf{H}_{(k,l)c} \mathbf{E}_{(i-k,j-l)c} \quad (1)$$

$$\bar{\mathbf{Y}}_{(i,j)} = \mathcal{Q}_c[\bar{\mathbf{U}}_{(i,j)}] \quad (2)$$

$$\text{and } \bar{\mathbf{E}}_{(i,j)} = \bar{\mathbf{Y}}_{(i,j)} - \bar{\mathbf{U}}_{(i,j)} = \mathcal{Q}_c[\bar{\mathbf{U}}_{(i,j)}] - \bar{\mathbf{U}}_{(i,j)} \quad (3)$$

where $\bar{\mathbf{U}}_{(i,j)}$ is a state vector of the system, $\bar{\mathbf{E}}_{(i,j)}$ is the quantization error of the pixel at position (i,j) and $\mathbf{H}_{(k,l)c}$ is a coefficient of the error diffusion filter for the c^{th} color component. S is the casual support region of $\mathbf{H}_{(k,l)c}$.

The operator $\mathcal{Q}_c[\bullet]$ performs a 3D vector quantization. During the operation, the 3D vector $\bar{\mathbf{U}}_{(i,j)}$ is compared with a set of vectors stored in a previously generated color palette $C = \{ \hat{\mathbf{v}}_i | i=1, \dots, N_c \}$. It is then represented by color $\hat{\mathbf{v}}_k \in C$ if and only if $\| \bar{\mathbf{U}}_{(i,j)} - \hat{\mathbf{v}}_k \| \leq \| \bar{\mathbf{U}}_{(i,j)} - \hat{\mathbf{v}}_j \|$ for all $j = 1, 2, \dots, N_c$. In other words,

we have $\bar{\mathbf{Y}}_{(i,j)} = \hat{\mathbf{v}}_k$. The index of the best-matched vector is recorded and the quantization error $\bar{\mathbf{E}}_{(i,j)} = \hat{\mathbf{v}}_k - \bar{\mathbf{U}}_{(i,j)}$ is diffused to pixel (i,j) 's neighborhood with eqn. (1). Note that, to handle the boundary pixels, $\bar{\mathbf{E}}_{(i,j)}$ is defined to be zero when (i,j) falls outside the image.

After the scanning is finished, the recorded indices can be used in the future to reconstruct the color-quantized image with the same color palette.

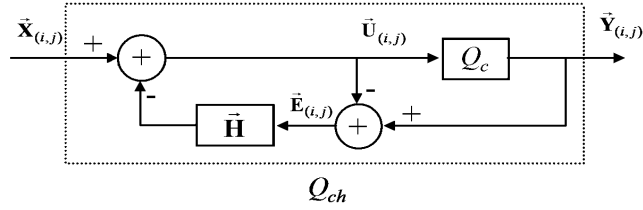


Figure 1. Color quantization with halftoning

3. CONSTRAINT SETS

The proposed algorithm is a POCS algorithm which makes an estimation of the original image \mathbf{X} with the observed \mathbf{Y} by projecting intermediate estimates among convex constraint sets iteratively. Suppose we have already made an estimation of \mathbf{X} to get an intermediate estimate \mathbf{X}' and are going to refine our estimate. The pixels of \mathbf{X}' are adjusted one by one in the refinement. The order of that the pixels are adjusted follows the order of that the pixels were color-quantized. Here, we assume that the degradation process Q_{ch} is known.

Without loss of generality, consider we are now processing pixel (m,n) . Since pixels are adjusted one by one as they were processed in color quantization, all previously adjusted pixels and pixel (m,n) of \mathbf{X}' form a partial image and can be color-quantized with operation Q_{ch} (eqns.(1-3)) until pixel (m,n) is reached. For the sake of reference, this partial image is referred to as \mathbf{I}_p hereafter. Let the set of the coordinates of the adjusted pixels and (m,n) be Ω_p . When \mathbf{I}_p is color-quantized with eqns.(1-3), intermediate state vectors $\bar{\mathbf{U}}_{(k,l)}$ and error vectors $\bar{\mathbf{E}}_{(k,l)}$, where $(k,l) \in \Omega_p$, are generated. They are referred to as $\bar{\mathbf{U}}'_{(k,l)}$ and $\bar{\mathbf{E}}'_{(k,l)}$.

Obviously, since $Q_{ch}[\bar{\mathbf{X}}_{(m,n)}] = \bar{\mathbf{Y}}_{(m,n)}$ must hold, a convex constraint set in which the desirable output image after adjusting pixel (m,n) should be can be formed as follows.

$$S_{2,(m,n)} = \{ \mathbf{I} \mid \bar{\mathbf{I}}_{(i,j)} = \bar{\mathbf{X}}'_{(i,j)} \quad \forall (i,j) \in \Omega_p \setminus (m,n), \\ \bar{\mathbf{I}}_{(i,j)} = \bar{\mathbf{X}}'_{(i,j)} \quad \forall (i,j) \notin \Omega_p \quad \text{and}$$

$$Q_{ch}[\bar{\mathbf{I}}_{(m,n)}] = \bar{\mathbf{Y}}_{(m,n)} \} \quad (4)$$

where $\bar{\mathbf{X}}'_{(i,j)}$ is the adjusted $\bar{\mathbf{X}}_{(i,j)}$ in the refinement, \mathbf{I} is an image whose size is the same as \mathbf{X} and $Q_{ch}[\bar{\mathbf{I}}_{(m,n)}]$ denotes the (m,n) th pixel of the output when image \mathbf{I} is processed with eqns.(1-3) from pixel (1,1) to pixel (m,n) .

Recall that $\bar{\mathbf{X}}'_{(m,n)}$ is the estimate of $\bar{\mathbf{X}}_{(m,n)}$ before adjustment. If $Q_{ch}[\bar{\mathbf{X}}'_{(m,n)}] = \bar{\mathbf{Y}}_{(m,n)}$ happens, the current state of the refined \mathbf{X}' will be a member of $S_{2,(m,n)}$ and no adjustment of $\bar{\mathbf{X}}'_{(m,n)}$ will be required.

However, it is possible that $Q_{ch}[\bar{\mathbf{X}}'_{(m,n)}] \neq \bar{\mathbf{Y}}_{(m,n)}$ as the $\bar{\mathbf{U}}'_{(m,n)}$ obtained with eqn.(1) is out of R_k as shown in Figure 2. In formulation, we have $Q_c[\bar{\mathbf{U}}'_{(m,n)}] \neq \bar{\mathbf{Y}}_{(m,n)}$. In such a case, a projection is necessary to project $\bar{\mathbf{U}}'_{(m,n)}$ onto the boundary of R_k . Starting from $\bar{\mathbf{U}}'_{(m,n)}$, we search along the straight line connecting $\bar{\mathbf{U}}'_{(m,n)}$ and $\bar{\mathbf{Y}}_{(m,n)}$ to seek a new point $\bar{\mathbf{U}}'_{(m,n)_{new}}$ such that $Q_c[\bar{\mathbf{U}}'_{(m,n)_{new}}] = \bar{\mathbf{Y}}_{(m,n)}$ is satisfied. The search is conducted with estimates generated iteratively with

$$\bar{\mathbf{U}}'_{(m,n)_{new}} = \bar{\mathbf{Y}}_{(m,n)} + \lambda^n (\bar{\mathbf{U}}'_{(m,n)} - \bar{\mathbf{Y}}_{(m,n)}) \quad (5)$$

where λ^n is a relaxation parameter at iteration n . The convergence of the estimate can be guaranteed as long as $0 \leq \lambda < 1$. After $\bar{\mathbf{U}}'_{(m,n)_{new}}$ is found, $\bar{\mathbf{U}}'_{(m,n)}$ is updated to be $\bar{\mathbf{U}}'_{(m,n)_{new}}$.

Note this point-to-point projection may not be perpendicular to the surface of R_k . However, this does not matter. One can define a plane which passes $\bar{\mathbf{U}}'_{(m,n)_{new}}$ and is perpendicular to the line connecting $\bar{\mathbf{U}}'_{(m,n)}$ and $\bar{\mathbf{Y}}_{(m,n)}$. This plane cuts through Voronoi region R_k and splits it into two. The one containing point $\bar{\mathbf{Y}}_{(m,n)}$ forms a new constraint set R_k' . By doing so, projection from $\bar{\mathbf{U}}'_{(m,n)}$ to $\bar{\mathbf{U}}'_{(m,n)_{new}}$ is equivalent to a projection onto a convex set R_k' .

After determining $\bar{\mathbf{U}}'_{(m,n)}$, the adjusted $\bar{\mathbf{X}}'_{(m,n)}$ can be obtained by

$$\mathbf{X}''_{(m,n)c} = \mathbf{U}'_{(m,n)c} + \sum_{(k,l) \in S} \mathbf{H}_{(k,l)c} \mathbf{E}'_{(m-k,n-l)c} \\ \text{for } c \in \{r, g, b\} \quad (6)$$

The adjusted image is then a member of $S_{2,(m,n)}$.

Typical images would generally have weak high frequency components as the intensity of neighboring pixels is highly correlated. This feature can be exploited as *a priori* information in the restoration of halftoned color-quantized images. In our approach, we assume that the energy of each high frequency component of \mathbf{X} is bounded as given by $|[T(\mathbf{X})]_{(u,w)}| \leq |[T(F(\mathbf{Y}))]_{(u,w)}|$ for $(u,w) \in \Omega_H$, where F and T are, respectively, a linear low-pass filtering operator and a 2D DCT operator, $[\bullet]_{(u,w)}$

denotes the $(u,w)^{th}$ element in the transform domain and Ω_H defines the set of high frequency components which should be bounded. This forms a smoothness constraint set

$$S_1 = \{ \mathbf{I} \mid |[T(\mathbf{I})]_{(u,w)}| \leq |[T(F(\mathbf{Y}))]_{(u,w)}| \text{ for } (u,w) \in \Omega_H \} \quad (7)$$

Another constraint set for restoring \mathbf{X} is the one that confines the intensity value of a particular pixel to be valid. In formulation, we have

$$S_3 = \{ \mathbf{I} \mid \bar{\mathbf{I}}_{(i,j)} \in \Gamma, \forall (i,j) \} \quad (8)$$

where $\Gamma = \{(r,g,b) \mid 0 \leq r,g,b \leq 1\}$.

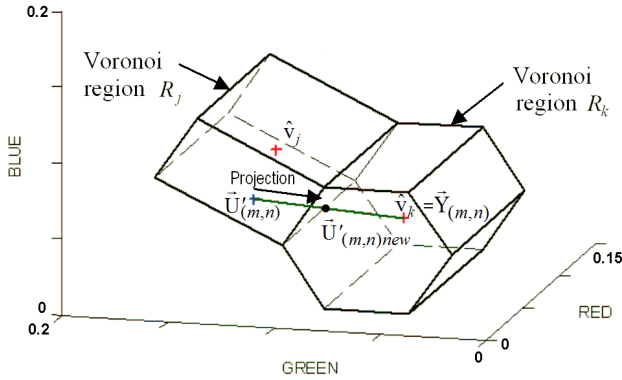


Figure 2. Projection of $\bar{\mathbf{U}}'_{(m,n)}$ onto R_k

4. PROJECTION ONTO CONVEX SETS

A POCS-based iterative algorithm can be defined based on the convex constraint sets defined in the previous Section. In formulation, we have

$$\mathbf{X}^{(m+1)} = P_3 P_{2,(N,N)} \cdots P_{2,(i,j)} \cdots P_{2,(1,1)} P_1 \mathbf{X}^{(m)} \quad (9)$$

where $\mathbf{X}^{(m)}$ is the estimate of \mathbf{X} at iteration m , and P_1 , $P_{2,(i,j)}$ and P_3 are, respectively, the projection operators to project a given image \mathbf{I} onto S_1 , $S_{2,(i,j)}$ and S_3 . In particular, they are defined as

$$P_1 : [T(\mathbf{I})]_{(u,w)} = [T(F(\mathbf{Y}))]_{(u,w)}$$

$$\text{if } |[T(\mathbf{I})]_{(u,w)}| > |[T(F(\mathbf{Y}))]_{(u,w)}| \text{ for } (u,w) \in \Omega_H \quad (10)$$

$$P_{2,(i,j)} : \mathbf{I}_{(i,j)c} = \begin{cases} \mathbf{I}_{(i,j)c} & \text{if } Q_c[\bar{\mathbf{U}}'_{(i,j)}] = \bar{\mathbf{Y}}_{(i,j)} \\ \mathbf{Y}_{(i,j)c} + \beta_{(i,j)}(\mathbf{U}'_{(i,j)c} - \mathbf{Y}_{(i,j)c}) + \sum_{(k,l) \in S} \mathbf{H}_{(k,l)c} \mathbf{E}'_{(i-k,j-l)c} & \text{if } Q_c[\bar{\mathbf{U}}'_{(i,j)}] \neq \bar{\mathbf{Y}}_{(i,j)} \end{cases} \text{ for } c \in \{r,g,b\}, \forall (i,j) \quad (11)$$

where $\beta_{(i,j)}$ is the corresponding λ^n for pixel (i,j) to adjust $\bar{\mathbf{U}}'_{(i,j)}$ with eqn.(5) such that $Q_c[\bar{\mathbf{U}}'_{(i,j)}] = \bar{\mathbf{Y}}_{(i,j)}$ can be satisfied.

$$P_3 : \mathbf{I}_{(i,j)c} = \begin{cases} 1 & \text{if } \mathbf{I}_{(i,j)c} > 1 \\ 0 & \text{if } \mathbf{I}_{(i,j)c} < 0 \end{cases} \text{ for } c \in \{r,g,b\}, \forall (i,j) \quad (12)$$

The initial estimate $\mathbf{X}^{(0)}$ is set to be $F(\mathbf{Y})$, although theoretically no restriction is imposed on the initial estimate. Since all constraint sets are convex sets, the convergence of POCS algorithm can be guaranteed.

5. SIMULATIONS

Simulation has been carried out to evaluate the performance of the proposed algorithm on a set of halftoned color-quantized images. In our simulation, a number of *de facto* standard 24-bit full color images including *Lenna*, *Baboon*, *Boat*, *Airplane*, *Peppers*, *Fruits*, *Couple*, *Girl* and *Tiffany* of size 256×256 each were used. For each image, a set of color palettes were generated with median cut algorithm [2] and their sizes varied from 16 to 128. Each testing image was then color-quantized with a palette to produce \mathbf{Y} . In color quantization, halftoning was performed with error diffusion and the Floyd-Steinberg diffusion filter [5] was used. The proposed restoration algorithm was applied to restore \mathbf{Y} . In the realization of the proposed algorithm, the 3×3 Gaussian filter was used as filter F . Ω_H and λ were, respectively, selected to be

$$\{(u,w) \mid (256-u)^2 + (256-w)^2 < 100000 \text{ and } 0 \leq u,w < 256\} \text{ and } 0.9.$$

For comparison, a recently proposed algorithm for restoring color-quantized images[15] was simulated. Besides, some other restoration algorithms [9,10,11] that were originally proposed for restoring noisy and blurred color images were also evaluated. In realizing the algorithms proposed in [9], [10] and [11], the noise power, the noise spectrum and the power spectrum of each color channel was estimated with the original full-color image. In a practical situation, no original image is available and hence all must be estimated from the degraded image. In other words, in practice, the restoration result of these algorithms may not as good as those presented in this paper. Besides, as it is not necessary for Fung's algorithm[15] and

the proposed algorithm to extract information with the original full-color image, additional credit should be added to these algorithms indeed.

The performance of the algorithms was evaluated as follows. For each color-quantized image Y generated with a particular testing image X , a restored output X' was obtained with a particular algorithm. The restoration result X' is evaluated in terms of SNR improvement and the CIELAB color difference (ΔE) metric[16]. The figures shown in Table 1 show the average values of the evaluation results of all standard testing images.

From Table 1a, one can see that the performance of the proposed algorithm is better as compared with the others. Here, the SNR improvement is defined as $SNRI=10\log(\|X-Y\|^2 / \|X-X'\|^2)$. The other algorithms do not take care of the halftoning process in restoring a color-quantized image and hence their performance is poor when halftoning is involved in the color quantization. The smaller the palette size, the more significant the effect of halftoning and hence the superiority of the proposed algorithm is more visible as compared with the other algorithms.

It is well accepted that color errors are visually detectable when $\Delta E > 3$ [11,17]. Table 1b shows the average of the ΔE values of all pixels in all restoration outputs and Table 1c shows the average of the percentage of pixels whose color error is visually undetectable in a restoration output. Again, one can see that the proposed algorithm is superior to the others.

	Palette size	Observed (Y)	Restored (X')					
			Ours	[15]	[11]-IND	[11]-KL	[9]	[10]
a			Average SNR Improvement (dB)					
	128	-	6.95	4.29	4.54	4.25	1.98	3.37
	64	-	8.51	4.63	5.29	4.96	2.85	4.15
	32	-	9.26	4.40	5.67	5.37	4.10	4.61
	16	-	8.72	3.84	5.15	4.97	3.52	4.43
b			Average of CIELAB difference ΔE					
	128	5.39	3.10	3.92	4.03	4.13	4.80	4.37
	64	6.64	3.61	4.88	4.82	4.98	5.68	5.26
	32	7.98	4.54	6.05	5.80	6.04	6.70	6.26
	16	9.86	6.39	8.10	7.54	7.76	8.92	7.83
c			% of pixels whose CIELAB $\Delta E < 3$					
	128	40.1	62.9	53.2	52.3	51.3	44.2	48.6
	64	30.7	57.4	43.3	43.9	42.5	35.5	40.0
	32	22.2	48.9	33.7	34.8	33.3	28.8	30.8
	16	14.7	35.1	22.8	24.9	23.9	18.7	24.5

Table 1. Average performance of various algorithms in restoring halftoned color-quantized images

6. CONCLUSIONS

In this paper we have introduced a restoration algorithm for restoring halftoned color-quantized images. This algorithm makes a good use of the available color palette and the halftoning process to derive useful *a priori* information for restoration. Simulation results

demonstrated that the proposed algorithm can achieve a better restoration performance in terms of both SNR and CIELAB color difference (ΔE) metric as compared with some other restoration algorithms.

7. ACKNOWLEDGEMENT

This work was supported by a grant from Centre for Multimedia Signal Processing, The Hong Kong Polytechnic University.

8. REFERENCE

- [1] M.T. Orchard and C.A. Bouman, "Color quantization of images," IEEE Trans. SP, Vol.39, pp.2677-2690, 1991.
- [2] P. Heckbert, "Color image quantization for frame buffer displays," Comput. Graph., Vol.16, No.4, pp. 297-307, 1982.
- [3] S.S. Dixit, "Quantization of color images for display/printing on limited color output devices," Comput.Graph., Vol. 15, No. 4, pp. 561-567, 1991.
- [4] X. Wu, "Color quantization by dynamic programming and principal analysis," ACM Trans. Graph., Vol. 11, No. 4, pp. 384-372, 1992.
- [5] R. Ulichney, *Digital Halftoning*. Cambridge, MA:MIT Press, 1987.
- [6] R.S. Gentile, E.Walowit, and J.P. Allebach, "Quantization and multi-level halftoning of color images for near original image quality," Proc. SPIE, Vol.1249, pp. 249-259, 1990.
- [7] M. Barni, V. Cappellini and L. Mirri, "Multichannel m-filtering for color image restoration," Proc., IEEE ICIP'2000, 2000, Vol.1, pp. 529-532.
- [8] G.Angelopoulos and I. Pitas, "Multichannel wiener filters in color image restoration," IEEE Trans. CASVT, Vol.4, pp.83-87, 1994
- [9] N.P. Galatsanos, A.K. Katsaggelos, R.T. Chin, and A.D. Hillery, "Least squares restoration of multichannel images," IEEE Trans. SP, Vol.39, pp.2222-2236, 1991.
- [10] B.R. Hunt and O.Kubler, "Karhunen-Loeve multispectral image restoration, Part 1: Theory," IEEE Trans. ASSP, Vol.32, pp.592-600, 1984.
- [11] H.Altunbasak and H.J. Trussell, "Colorimetric restoration of digital images," IEEE Trans. IP, Vol.10, pp.393-402, 2001.
- [12] K.J. Boo and N.K. Bose, "Multispectral image restoration with multisensor," IEEE Trans. Geoscience and Remote Sensing, Vol.35, pp.1160-1170, 1997.
- [13] N.P. Galatsanos and R.T. Chin, "Digital restoration of multichannel images," IEEE Trans. ASSP, Vol.37, pp. 415-421, 1989.
- [14] N.P. Galatsanos and R.T. Chin, "Restoration of color images by multichannel Kalman filtering," IEEE Trans. SP, Vol.39, pp.2237-2252, 1991.
- [15] Y.H. Fung and Y.H. Chan, "An Iterative Algorithm for Restoring Color-Quantized Images," Proceedings, IEEE ICIP'02, 2002, Vol.1, pp.313-316.
- [16] C.I.E. (1978) Recommendations on uniform color spaces, color difference equations, psychometric color terms. Supplement No.2 to CIE publication No.15 (E.-1.3.1) 1971/(TC-1.3.).
- [17] C. Connolly, T.W.W. Leung and J. Nobbs, "Colour measurement by video camera," JSDC, Vol. 111, pp. 373-375, 1995.